International Journal of Current Microbiology and Applied Sciences
ISSN: 2319-7706 **Volume 3 Number 4 (2014) pp. 374-383**
http://www.ijcmas.com

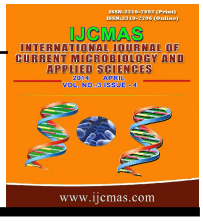

Original Research Article

Green Synthesis of Silver Nanoparticles of different Shapes and its Antibacterial Activity against *Escherichia coli*

Anandini Rout[1], Padan K. Jena[1], Debasish Sahoo[2] and Birendra K.Bindhani[2]*

[1]Department of Botany, Ravenshaw University, Cuttack, Odisha, India
[2]School of Biotechnology, KIIT University, Bhubaneswar, Odisha, India
Corresponding author

A B S T R A C T

In this investigation, the antibacterial activities of silver nanoparticles of different shapes (i.e., Spherical, Triangular and Rod) were synthesized by using Mulberry (*Morus rubra* L.) leaves extract against *Escherichia coli* in both liquid systems and on agar plates. The syntheisised nanoparticles were characterized by UV – Visible spectroscopy, X-Ray Diffraction (XRD) and Transmission Electron Microscopy (TEM). The growth or killing kinetics of bacteria treated with silver nanoparticles was studied against *Escherichia coli* by using Pro 7.5 software. In liquid medium treated with silver nanoparticles at high concentrations showed delay growth of *Escherichia coli*. A high reactivity of the truncated triangular nanoplates was observed in comparison to other particles like spherical or rod-shaped particles. Hence, these findings provide a base for the measurement of shape dependent bacterial activity of silver nanoparticles.

K e y w o r d s

Green Synthesis, Antibacterial Activity, Silver Nanoparticles, Mulberry (*Morus rubra* L.).

Introduction

In recent times, precious metal nanoparticles (i.e., Gold Nanoclusters (AgNCs)) are extremely attractive because of their high fluorescence, good photostability, non-toxicity, excellent biocompatibility and solubility. The biomimetic synthesis has become a promising green pathway to prepare nanomaterials. Over the past few decades, inorganic nanoparticles, whose structures exhibit significantly novel and improved physical, chemical, and biological properties, phenomena, and functionality due to their nanoscale size, have elicited much interest. Nanophasic and nanostructured materials are attracting a great deal of attention because of their potential for achieving specific processes and selectivity, especially in biological and pharmaceutical applications (Faramarzi *et al*., 2013; Anandhakumar *et al*., 2011). Discoveries in the past decade have demonstrated that the electromagnetic, optical, and catalytic properties of noble-metal nanocrystals are strongly influenced by shape and size (Clemens *et al*., 2005; Mulvaney, 1996). This has motivated an upsurge in research on the synthesis routes that allow better

control of shape and size (Nikil *et al*., 2001; Yugang *et al.*, 2003 and Zhou *et al.*, 1999), with projected applications in nanoelectronics and spectroscopy (Kevin *et al*., 2001; Knoll *et al*., 1999; Peter *et al*., 2000).

The latest studies have demonstrated that specifically formulated metal oxide nanoparticles have good antibacterial activity (Wei *et al*., 2014) and antimicrobial formulations comprising nanoparticles could be effective bactericidal materials (Xiang *et al.*, 2012; Tarek *et al.*, 1999). Amongst inorganic antibacterial agents, silver has been employed most extensively since ancient times to fight infections and control spoilage. The antibacterial and antiviral actions of silver, silver ion, and silver compounds have been thoroughly investigated (Hiroaki *et al*., 1994; Oloffs *et al*., 1994; Tokumaru *et al*., 1974). However, in minute concentrations, silver is nontoxic to human cells. The epidemiological history of silver has established its nontoxicity in normal use. Catalytic oxidation by metallic silver and reaction with dissolved monovalent silver ion probably contribute to its bactericidal effect (James, 1971). Microbes are unlikely to develop resistance against silver, as they do against conventional and narrow-target antibiotics, because the metal attacks a broad range of targets in the organisms, which means that they would have to develop a host of mutations simultaneously to protect themselves. Thus, silver ions have been used as an antibacterial component in dental resin composites (Herrera *et al*., 2001), in synthetic zeolites (Yoshinobu *et al*., 2003) and in coatings of medical devices (Bosetti *et al*., 2002).

However, little is known about how the biological activity of silver nanoparticles changes as the shape of the particles changes. For these reason, we investigated the shape dependence of the antibacterial activity of silver nanoparticles against *Escherichia coli*. Silver nanoparticles of different shapes were synthesized by solution phase routes, and their interactions with *E. coli* were studied. Transmission electron microscopy was used as a complementary technique to examine the treated cells. The size-dependent antimicrobial activity of silver nanoparticles has already been investigated (Ping *et al*., 2005; Ivan *et al*., 2004; Jose *et al.*, 2005 and Jose *et al*., 2005), while to our knowledge the effect of shape on the antibacterial activity of silver nanoparticles has not been reported previously.

Materials and Methods

Materials:

Escherichia coli (MTCC 10312) was obtained from the Microbial Type Culture Collection and Gene Bank (IMT, Chandigarh, India). The bacterial cultures were grown and maintained as per the supplier's protocol. Other chemicals like silver nitrate, ascorbic acid, sodium citrate tribasic dihydrate and cetyltrimethyl ammonium bromide (CTAB) were obtained from Himedia, India.

Preparation of the Extract:

Weighing 25g of Mulberry (*Morus rubra* L.) leaves was thoroughly washed in distilled water, dried, cut into fine pieces and was smashed into 100 ml sterile distilled water and filtered through Whatman No.1 filter paper. The extract was stored at 4°C for further experiments.

Synthesis of Silver Nanoparticles from Mulberry Leaves Extract:

The aqueous solution of 1mM silver nitrate ($AgNO_3$) was prepared and used for the synthesis of silver nanoparticles. Then, 10 ml of Mulberry (*Morus rubra* L.) leaves extract was added into 90 ml of aqueous solution of 1 mM silver nitrate for reduction into Ag^+ ions and kept for incubation period of 15h at room temperature. Here the filtrates act as reducing and stabilizing agent for 1 mM of $AgNO_3$.

In the first method, the spherical silver hydrosols were prepared by reducing aqueous $AgNO_3$ with sodium citrate at near-boiling temperature. In a typical procedure, an aqueous solution of $AgNO_3$ (100 ml, 0.001 M) was brought to boiling, and then 3 ml of the silver seed solution and an aqueous solution of sodium citrate were added so that the final concentration of sodium citrate in the reaction mixture became 0.001 M. The solution was heated until the colour was greenish yellow. The solution was cooled to room temperature. The silver nanoparticles were purified by centrifugation. To remove excess silver ions, the silver pellet was washed three times with deionized water. A dried powder of the nanosize silver was obtained by freeze-drying. To carry out interaction of the silver nanoparticles with bacteria, the silver nanoparticle powder in the freeze drying cuvette was re-suspended in water; the suspension was homogenized with a Branson 2200 ultrasonicator.

Rod-shaped (Elongated) and truncated triangular silver nanoplates were synthesized by a solution phase method for the large-scale preparation of truncated triangular nanoplates (Sihai *et al*., 2002). To the particle growth solution containing 5 ml of 0.01 M$AgNO_3$, 10 ml of 0.1 M ascorbic acid, 146 ml of 0.1 MCTAB, and 5 ml of silver seeds, 1 ml of 1 M NaOH was added to accelerate particle growth. The solution colour changed from light yellow to brown, red, and green within a few minutes. The resultant solution was aged at 21°C for 12 h, 35°C for 5 min, and 21°C for 24 h. The colour of the aged solution changed from green to red. The silver nanoplates were purified by centrifugation. The surfactants and the smaller particles were separated by centrifugation at 2,100 X g for 10 min. The resultant precipitate was suspended in water and centrifuged again at 755 X g for 10 min. Finally, the precipitate was suspended in water, and rods with larger aspect ratios were removed by centrifuging at 84 X g for 10 min. The supernatant solution contained the truncated triangular silver nanoplates. It was not possible to quantify the precipitate by weight, as it was always associated with some water.

Organism Preparation

Escherichia coli MTCC 10312 was grown overnight in NB at 37°C. Washed cells were re-suspended in NB, and optical density (OD) was adjusted to 0.1, corresponding to 108 CFU/ml at 600 nm.

Bacterial Growth or Killing Kinetics in Presence of Nanosilver

To examine the bacterial growth or killing kinetics in the presence of silver nanoparticles, *Escherichia coli* cells were grown in 100 ml of NB supplemented with different doses of nanosilver (total silver content, 1 µg, 6 µg, 12 µg, 12.5 µg, 50 µg, or 100 µg), at 37°C with continuous agitation. The cylindrical sample containers were placed horizontally on an orbital

shaker platform and agitated at 225 rpm. Growth or killing rates and bacterial concentrations were determined by measuring OD at 600 nm. The OD values were converted into concentration of *Escherichia coli* cells (CFU per milliliter) (Ping *et al.*, 2005; Ivan *et al*., 2004).

Characterization of Silver Nanoparticles

The synthesized nanoparticles were characterized by UV-visible spectroscopy and TEM. TEM images were observed with a LIBRA 120 (Carl Zeiss) transmission electron microscope. The samples were prepared by placing a drop of homogeneous suspension on a copper grid with a lacey carbon film and allowing it to dry in air. Mean particle size was analyzed from the digitized images with Image Tool software. UV-visible absorption spectra were recorded with an Optizen 2120 UV-visible spectrophotometer (Mecasys, Daejeon, Korea) with a 1-cm quartz cell.

Results and Discussion

UV-visible Spectroscopy

UV-visible spectroscopy is one of the most widely used techniques for structural characterization of silver nanoparticles. The absorption spectrum (Fig. 1) of the pale yellow silver colloids prepared by citrate reduction showed a surface plasmon absorption band with a maximum of ~420 nm, indicating the presence of lone spherical or roughly spherical Ag nanoparticles.

The optical absorption spectra of metal nanoparticles are dominated by surface plasmon resonances (SPR), which shift to longer wavelengths with increasing particle size (Jose *et al.*, 2005; Jose *et al.*, 2005; Sihai *et al*., 2002; Ivan *et al*., 2003; Brause *et al*., 2002). The position and shape of plasmon absorption of silver nanoclusters are strongly dependent on the particle size, dielectric medium, and surface-adsorbed species (Kreibig *et al*., 1995; Mulvaney, 1996).

According to Mie's theory (Kreibig *et al*., 1995; Mie, 1908), only a single SPR band is expected in the absorption spectra of spherical nanoparticles, whereas anisotropic particles could give rise to two or more SPR bands depending on the shape of the particles. The number of SPR peaks increases as the symmetry of the nanoparticle decreases (Ivan *et al.*, 2003). Thus, spherical nanoparticles, disks, and triangular nanoplates of silver show one, two, and more peaks, respectively. Even after several days, the aqueous dispersion of freeze dried Ag nanoparticles, prepared by citrate reduction, displayed UV-visible spectral characteristics of spherical Ag nanoparticles (Fig. 1), confirming the colloidal stability and uniformity of the silver hydrosol.

TEM

The TEM image (Fig. 2) confirmed that a minimum at ~420 nm corresponds to the wavelength at which the real and imaginary parts of the dielectric function of silver almost vanish (Schatz *et al*., 2002; Yugang *et al*., 2003; Jasmina *et al*., 2002; James *et al*., 2000; Callegari *et al*., 2003; Feng *et al*., 2000; Ivan *et al*., 2003).

Further, TEM images (Fig. 2) revealed more significant differences between these samples in terms of particle morphology. While samples prepared by citrate reduction consisted mostly of spherical

Figure.1 Showing Absorption Spectra of solutions containing spherical silver nanoparticle recorded instantly after precipitation and after one week

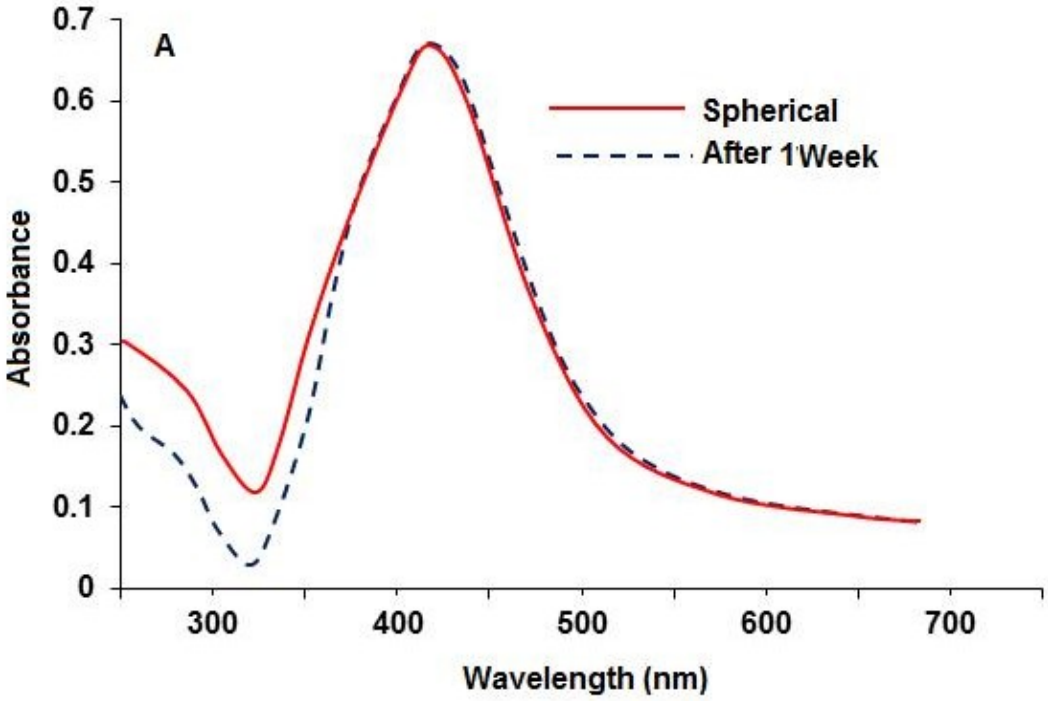

Figure.2 Showing different TEM images of silver nanoparticles (A) Spherical nanoparticles (B) Silver nanoparticles of different shapes. (C) Rod-shaped nanoparticles.

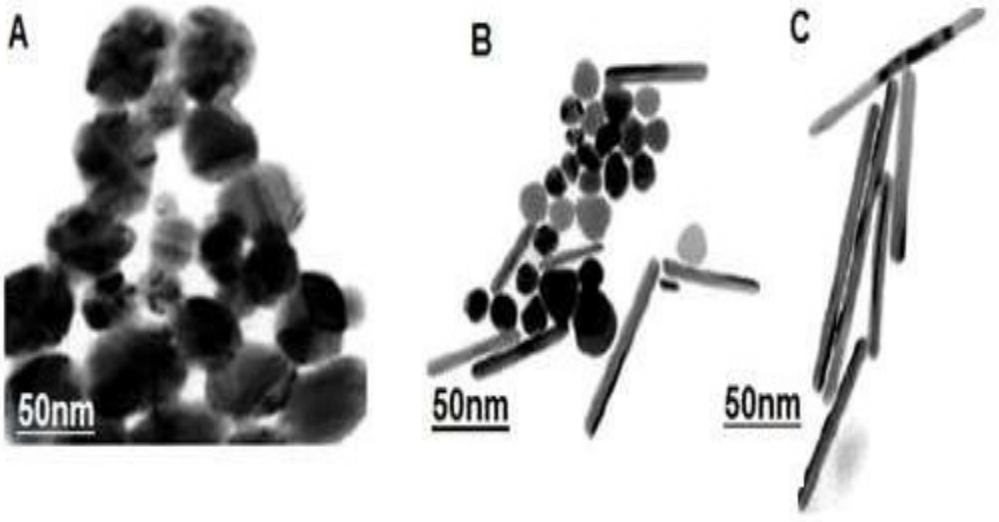

Figure.3 Showing XRD pattern of truncated triangular silver nanoplates

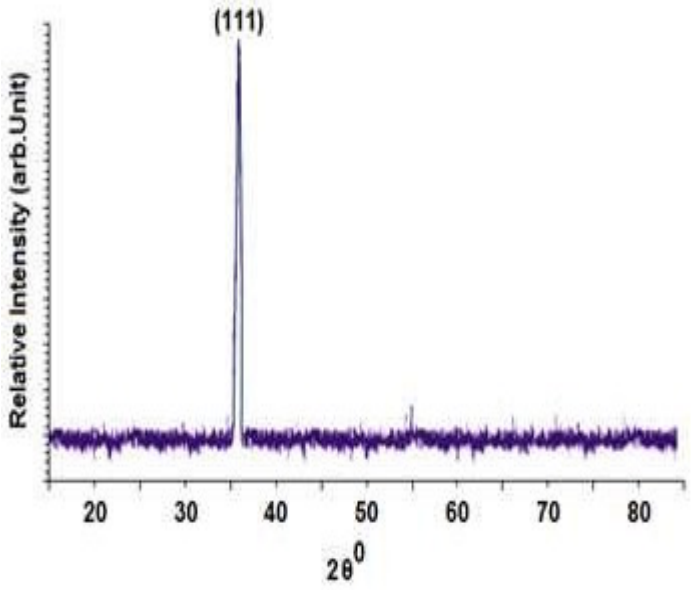

Figure.4 Showing number of *Escherichia coli* colonies, expressed in log as a function of the amount of silver nanoparticles in agar plates

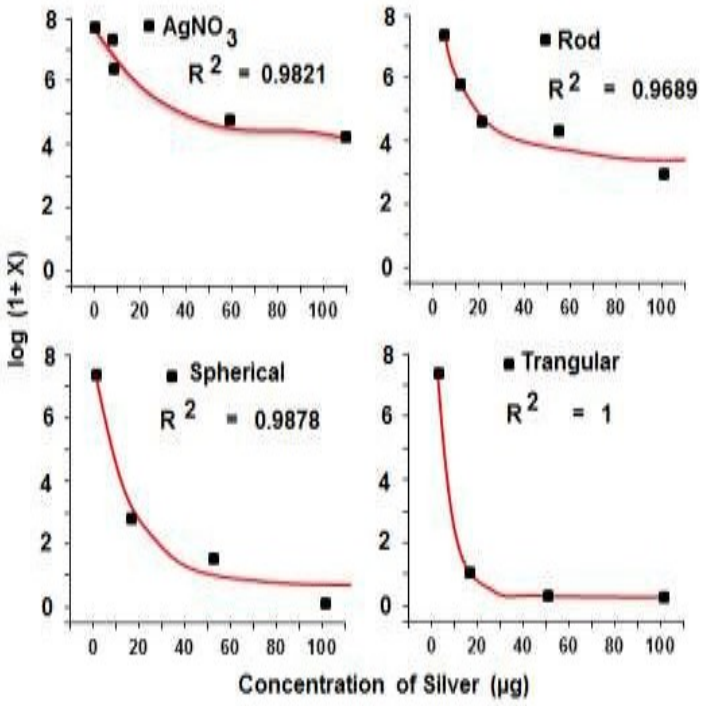

Figure.5 (A) Ag^{+} (in the form of $AgNO_3$) & (B) Spherical silver nanoparticles. Petri dishes at first supplemented with 105 CFU/ml of *Escherichia coli* and incubated with silver at (a) 1 µg, (b) 6 µg, (c) 12.5 µg, (d) 50 µg, and (e) 100 µg and corresponding graphs showing log (1 + number of colonies grown on plates) as a function of the concentration of silver in agar plates.

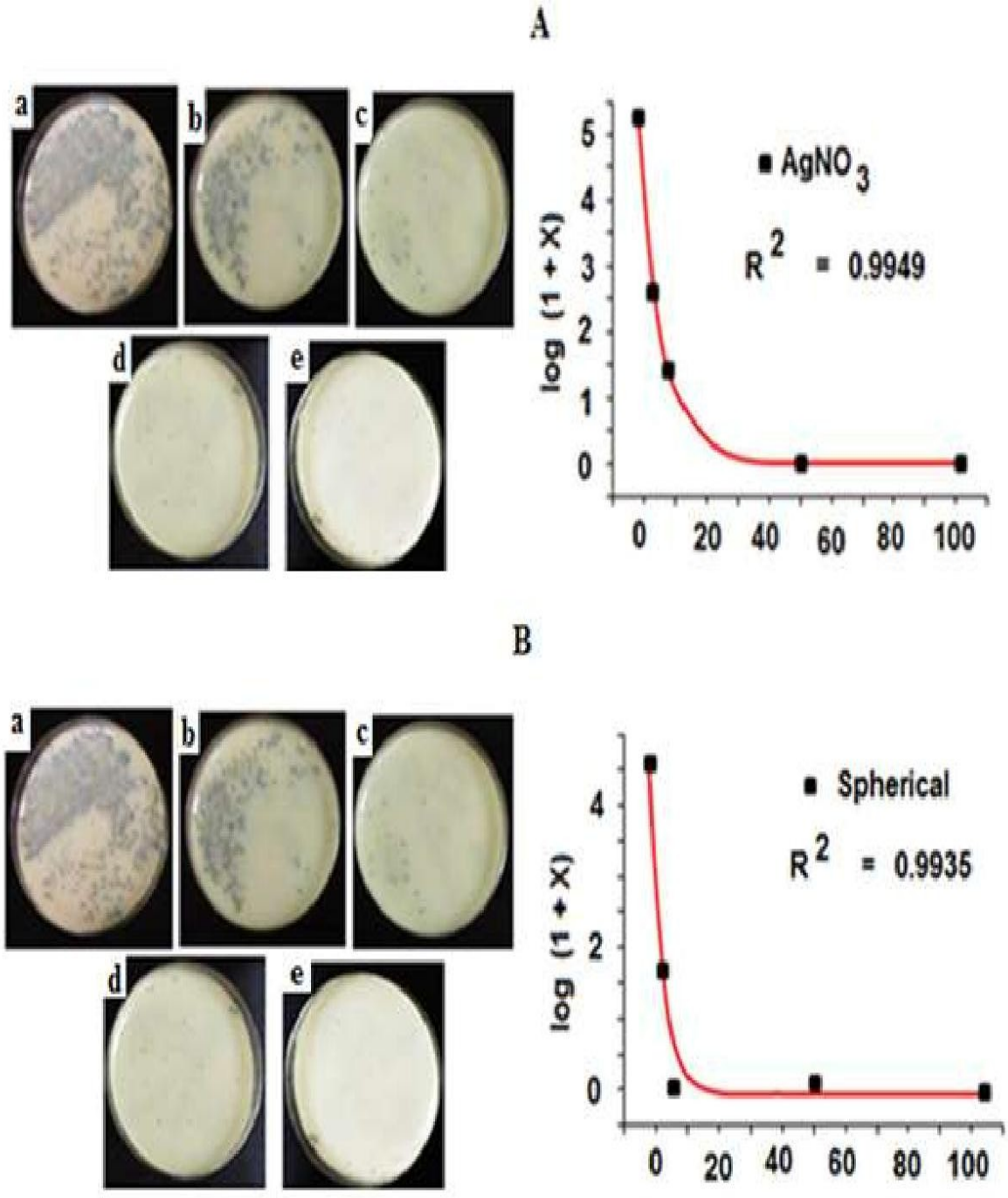

nanoparticles (Fig. 2A), anisotropic Ag particles (truncated triangular plates, rods, and polyhedral plates) were more easily identified in other samples (Fig. 2B and C).

X-Ray Diffraction (XRD)

Structural information on the truncated triangular nanoplates was obtained by X-ray diffraction (XRD). In Figure 3 showed the XRD patterns of the nanoplates lying flat with their basal planes parallel to the substrate. The remarkably intensive diffraction peak at a 2θ value of 38.04 from the [111] lattice plane of face-centered cubic silver unequivocally indicates that the particles are made of pure silver and that their basal plane, i.e., the top crystal plane, should be the [111] plane (Mikihiro *et al*., 2005; Sihai *et al*., 2002). It has been suggested (Bragg *et al*., 1974; Sihai *et al*., 2002) that this plane may possess the lowest surface tension. In Figure 3 showed the TEM image of purified truncated triangular particles with an average edge length of 50 nm.

In Figure 4 showed the corresponding results, expressed as log $(1 + x) = f(c)$, i.e., log $(1 + x)$ as a function of the total amount of silver nanoparticles (c), where x was the number of CFU grown on agar plates. The decrease in number of viable cells with increasing amounts of silver can be fitted with a first-order exponential decay curve with a nonlinear regression coefficient (R^2) ranging from 0.96 to 1. In Figure 5 displayed the number of bacterial colonies grown in the presence of different amount of $AgNO_3$ and spherical nanoparticles when 100 µl (approximately 10^5 CFU/ml) of sample was applied to each plate. The results clearly indicate that at a given concentration of silver, inhibition of bacterial growth depends on the initial number of cells. An amount of 6 µg of spherical nanoparticles almost completely prevented bacterial growth (Figure 5B). At silver (in the form of $AgNO_3$) amounts of 12.5 µg and above, 100% inhibition of bacterial growth was also observed (Figuer 5A). This is markedly different from the results obtained when the initial number of bacterial cells was 10^7 CFU. In this case also, the results, expressed as log $(1 + x) = f(c)$, follow the first-order exponential decay curve with a nonlinear regression coefficient (R^2) of ~0.99 (Figure 5).The bacterial growth kinetics was monitored in 100 ml NB medium (initial bacterial concentration, 10^7 CFU/ml) supplemented with different amounts of different silver nanoparticles Bragg *et al*., 1974; Gerald *et al*., 1999; Benjamin *et al*., 2005; Ajayan *et al*., 1988; David *et al*., 1996).

In the present study, it may be postulated that silver nanoparticles with the same surface areas but with different shapes may also have different effective surface areas in terms of active facets. Our finding provide a basis for the measurement of shape dependent bacterial activity of silver nanoparticles though at present it is unable to give an estimation of how the surface areas of different nanoparticles influence their killing activity or to relate the bacterial killing capacity of silver nanoparticles with their effective surface areas. However, it is very important that the flexibility of nanoparticle preparation methods and their influence on other bacterial strains be explored.

Acknowledgement

The authors are grateful to Department of Botany, Ravenshaw University, Cuttack,

Odisha, India and School of Biotechnology, KIIT University, Bhubaneswar, Odisha, India for providing necessary laboratory facilities for this investigation.

References

Ajayan, P. M., and Marks, L. D. 1988. Quasimelting and phases of small particles. Phys. Rev. Lett. 60 7:585–587.

Anandhakumar, S. and Raichur, A. M. 2011. A facile route to synthesize silver nanoparticles in polyelectrolyte capsules. Colloids Surf B Biointerfaces. 842:379-83.

Benjamin, W., Yugang, S. D., Brian, M. D. and Younan, X. P. 2005. Shape-controlled synthesis of metal nanostructures: the case of silver. Chem. Eur. J. 11 2:454–463.

Bosetti, M., Masse, A., Tobin, E. and Cannas, M. 2002. Silver coated materials for external fixation devices: in vitro biocompatibility and genotoxicity. Biomaterials. 23:887– 892.

Bragg, P. D., and Rainnie, D. J. 1974. The effect of silver ions on the respiratory chains of

Escherichia coli. Can. J. Microbiol. 20 6:883–889.

Brause, R., Moeltgen, H. and Kleinermanns, K. 2002. Characterization of laser-ablated and chemically reduced silver colloids in aqueous solution by UV/VIS spectroscopy and STM/SEM microscopy. Appl. Phys. 75 6-7:711–716.

Callegari, A., Tonti, D. and Chergui, M. 2003. Photochemically Grown Silver Nanoparticles with Wavelength-Controlled Size and Shape. Nano Lett. 3 11:1565– 1568.

Clemens, B., Xcaobo, C., Radha, R. and Mostafa, A.E.S. 2005. Chemistry and properties of nanocrystals of different shapes. Chem. Rev. 105:1025–1102.

David, W. H. and Henry, S. W. 1996. Electrochemistry of sulfur adlayers on the low-index faces of silver. J. Phys. Chem. 100 23:9854–9859.

Faramarzi, M. A. and Sadighi, A. 2013. Insights into biogenic and chemical production of inorganic nanomaterials and nanostructures Adv Colloid Interface Sci. 189-190:1-20.

Feng, Q. L., Wu, J., Chen, G. Q., Cui, F. Z., Kim, T. M., and Kim, J. O. 2000. A mechanistic study of the antibacterial effect of silver ions on *Escherichia coli* and *Staphylococcus aureus*. J. Biomed. Mater. Res. 52:662–668.

Gerald, M. D. and Denver, R. 1999. Antiseptics and disinfectants: activity, action, and resistance. Clin. Microbiol. 12:147–179.

Herrera, M., Carrion, P., Baca, P., Liebana, J. and Castillo, A. 2001. In vitro antibacterial activity of glass-ionomer cements. Microbios. 104:141–148.

Hiroaki, O., Toshikazu, T., Katsumi, T., Atsushi, N., and Shigeharu, U. 1994. Inactivation of enveloped viruses by a silver-thiosulfate complex. Metal-Based Drugs. 1:511.

Ivan, S. and Branka, S. S. 2004. Silver nanoparticles as antimicrobial agent: a case study on

E. coli as a model for Gram-negative bacteria. J. Colloid Interface Sci. 275: 177–182.

Ivan, O. S., Cecila N. and Ruben, G. B. 2003. Optical Properties of Metal Nanoparticles with Arbitrary Shapes. J. Phys. Chem. 107 26:6269–6275.

James, G. V. 1971. Water treatment: A survey of current methods of purifying domestic supplies and of treating industrial effluents and domestic sewage. 4th ed., p. 38. CRC Press, Cleveland, OH.

James, P. N. and Daniel, L. F. 2000. Assembly of Phenylacetylene-Bridged Silver and Gold Nanoparticle Arrays. J. Am. Chem. Soc. 12216: 3979–3980.

Jasmina, H., Nada M. D., Gregory, A. W., and Gary, P. W. 2002. Photoinduced Charge Separation Reactions of J-Aggregates Coated on Silver Nanoparticles. J. Am. Chem. Soc. 124 17:4536–4537.

Jose, L. E., Justin, L. B., Jose, R. M., Alejandra, C. B., Xiaoxia, G., Humberto, H. L. and Miguel, J. Y. 2005. Interaction of silver nanoparticles with HIV-1. J. Nanobiotechnol. 3:6.

Jose, R. M., Jose. L. E., Alejandra, C., Katherine, H., Juan, B. K., Jose, T. R. and Miguel, J. Y. 2005. The bactericidal effect of silver nanoparticles. Nanotechnology. 16:2346– 2353.

Kevin, D. H., Simon, O. L., Jacob, P. W., Eric, W. K. and Orlin, D. V. 2001. Dielectrophoretic Assembly of Electrically Functional Microwires from Nanoparticle Suspensions. Science. 294:1082–1086.

Knoll, B. and Keilmann, F. 1999. Near-field probing of vibrational absorption for chemical microscopy. Nature. 399:134–137.

Kreibig, U., and Vollmer, M. 1995. Optical properties of metal clusters. Springer, Berlin, Germany.

Mikihiro, Y., Keita, H., and Jun, K. 2005. Bactericidal Actions of a Silver Ion Solution on *Escherichia coli*, Studied by Energy-Filtering Transmission Electron Microscopy and Proteomic Analysis. Appl. Environ. Microbiol. 71 11:7589–7593.

Mie, G. 1908. Contributions to the optics of turbid media, especially colloidal metal solutions. Ann. Phys. 25:377–445.

Mulvaney, P. 1996. Surface Plasmon spectroscopy of nanosized metal particles. Langmuir. 12:788–800.

Nikil, R. J., Latha, G., and Catherine, J. M. 2001. Wet chemical synthesis of high aspect ratio cylindrical gold nanorods. J. Phys. Chem. 105:4065– 4067.

Oloffs, A., Crosse-Siestrup C., Bisson S., Rinck M., Rudolvh, R. and Gross, U. 1994. Biocompatibility of silver-coated polyurethane catheters and silver-coated Dacron® material. Biomaterials. 15:753–758.

Peter, M. T., Orlin, D. V., Anand, T. K., John, F. R., Abraham, M. L. and Eric, W. K. 2000. Assembly of Gold Nanostructured Films Templated by Colloidal Crystals and Use in Surface-Enhanced Raman Spectroscopy. J. Am. Chem. Soc. 122: 9554–9555.

Ping, L., Juan L., Changzhu, W., Qingsheng, W. and Jian, L. 2005. Synergistic antibacterial effects of ß-lactam antibiotic combined with silver nanoparticles. Nanotechnology. 16:1912–1917.

Schatz, G. C., and R. P. Van Duyne. 2002. Electromagnetic mechanism of surface-enhanced spectroscopy, p. 759–774. *In* J. M. Chalmers and P. R. Griffiths ed., Handbook of vibrational spectroscopy. Wiley, New York, NY.

Sihai, C. and David, L. C. 2002. Synthesis and Characterization of Truncated Triangular Silver Nanoplates. Nano Lett. 2 9:1003–1007.

Tarek, H., Michael, M. H., Zhengyi, C., Richard, T., Kent, J., Craig, W., Joan, B., and James, R. B. 1999. A novel surfactant nanoemulsion with broad-spectrum sporicidal activity against Bacillus species. J. Infect. Dis. 180:1939–1949.

Tokumaru, T., Shimizu, Y. and Fox, C. L. 1974. Antiviral activities of silver sulfadiazine and ocular infection. Res. Commun. Chem. Pathol. Pharmacol. 8:151–158.

Wei, X., Weiping, J., Liufeng, L., Chunlan, Z., Zhenshun, L., Yan, L., Rong, S. and Bin, L. 2014. Green synthesis of xanthan conformation-based silver nanoparticles: antibacterial and catalytic application. Carbohydr Polym. 101: 961-7.

Xiang, F., Minghui, J., Xin D., Yuhong, Y., Ren Z., Zhengzhong, S., Xia Z. and Xin, C. 2012. Green synthesis of silk fibroin-silver nanoparticle composites with effective antibacterial and biofilm-disrupting properties. Biomacromolecules. 14 12 : 4483-4488

Yoshinobu, M., Kuniaki Y., Shinichi, K. and Tetsuaki, T. 2003. Mode of Bactericidal Action of Silver Zeolite and Its Comparison with That of Silver Nitrate. Appl. Environ. Microbiol. 69: 4278–4281.

Yugang, S., Brian M. and Younan, X. 2003. Transformation of Silver Nanospheres into Nanobelts and Triangular Nanoplates through a Thermal Process. Nano Lett. 3 5: 675–679.